FURTHER INVESTIGATIONS ON THE MESA INJECTOR*

R. Heine†, K. Aulenbacher, S. Friederich, C. Matejcek, F. Schlander
Institut für Kernphysik, Johannes Gutenberg-Universität Mainz, Mainz, Germany

Abstract

The MESA ERL (**M**ainz **E**nergy-recovering **S**uperconducting **A**ccelerator) to be built at Mainz in the next years is a multi turn recirculating linac with beam currents of up to 10 mA. The dynamic range of the beam currents demanded by the experiments is of at least two orders of magnitude. This is a special challenge for the layout design of the injector. In this paper we present the current status of the design of the injector linac called MAMBO (**M**illi**AM**pere **BO**oster).

INTRODUCTION

MESA will be operated in two modes: the first is the external beam (EB) mode; there the beam is dumped after being used with the external fixed target experiment P2. The current required for P2 is 150 μA with polarised electrons at 155 MeV. The second mode is energy recovery (ER). The experiment served in this mode is an (pseudo) internal fixed target experiment named MAGIX. It demands an unpolarised beam of 1 mA at 105 MeV. In a later stage the ER-mode current shall be upgraded to 10 mA.

The concept of MAMBO was presented in [1]. MAMBO consists of a low energy beam transport (LEBT) section preparing a 100 keV beam with a chopper buncher system for capture in the first linac RF-section. The electrons are provided by a 100 keV DC photo gun that is driven by a pulsed laser. Although the laser pulses will last some 200 ps, delayed emission of electrons and dark currents make a chopper system necessary to cut off tails.

The electrons are accelerated by four room temperature RF-sections to 5 MeV. The frequency is determined by the SRF structures of the main linac, which are using TESLA technology at 1.3 GHz. The normal conducting structures are bi-periodic $\pi/2$ standing wave structures. The first section is a graded-β, the 2nd section has a constant $\beta < 1$ and the last two sections are $\beta = 1$. The geometry of the cells is derived from the MAMI injector [2].

BEAM DYNAMICS

The beam dynamics was simulated with PARMELA [3]. To receive more realistic results the space charge mesh was improved to allow for a changing bunch spacing due to energy gain. Especially inside a graded-β section the distance between bunches changes from cell to cell. This was modelled by using the `continue` command followed by a `scheff` line with altered mesh data. Further the number of particles was increased to 300,000 to allow for halo effects to become visible. Also now the 3D space charge functionality of PARMELA is used.

While arranging focussing elements, now spacial constraints, e.g. positions of flanges, are considered leading to minor alteration in their positions.

Table 1: Bunch Data at the Start of LEBT (i) and at the Exit of MAMBO (f)

		stage -1		stage - 2
I_b	[mA]	0.15	1	10
$\Delta\phi_i$(100%)	[°]	93.6	93.6	93.6
ΔT_i(100%)	[keV]	0.002	0.13	1.1
$\Delta\phi_f$ (RMS)	[°]	0.14	0.36	1.9
ΔT_f (RMS)	[keV]	0.85	2.2	5
$\Delta T_f/T$ (RMS)	$\times 10^{-4}$	1.7	4.4	10

The particle distribution now used for simulation has been extracted from CST Particle Studio [4] simulations of the photo source at a given bunch length (see Table 1). The phase spaces achieved with the linac configuration meet the design goals of MAMBO stage-1 ($\Delta\varphi \leq 3°$, $\Delta T/T = O(10^{-4})$) [1]. The parameters of stage-2 will not meet these goals, since space charge forces lead to an energy blow-up right from the gun. The energy spread achieved by MAMBO at 10 mA is 10^{-3}. The most demanding experiment P2 will be satisfied with the results for 150 μA, while MAGIX, which is asking for high currents, can cope with larger energy spread, so stage-2 parameters should be acceptable. This has to be investigated within the design of the main linac.

Space charge calculations also revealed that it is not possible to accelerate 10 mA inside the first RF-section without additional focussing applied over this section. Further an increase of the beam hole diameter in the iris seems to be advantageous.

RF-DESIGN

The MAMI structure has been scaled to 1.3 GHz and some modifications have been made to increase the coupling between cells, this will provide a better field flatness. Compared to the MAMI profile the coupling slots have been moved outside, this increases the area of the slots and therefore the coupling. To close the passband gap, the radius of the coupling cells was reduced. To allow for emittance blow up due to space charge the beam pipe diameter was increased on cost of ca. 10% of shunt impedance. The alterations of MAMBO structure compared to MAMI Ilac are visible in Fig. 1.

* Work supported by the German Federal Ministry of Education and Research and German Science Foundation under the Cluster of Excellence "PRISMA"

† rheine@uni-mainz.de

ISBN 978-3-95450-168-7

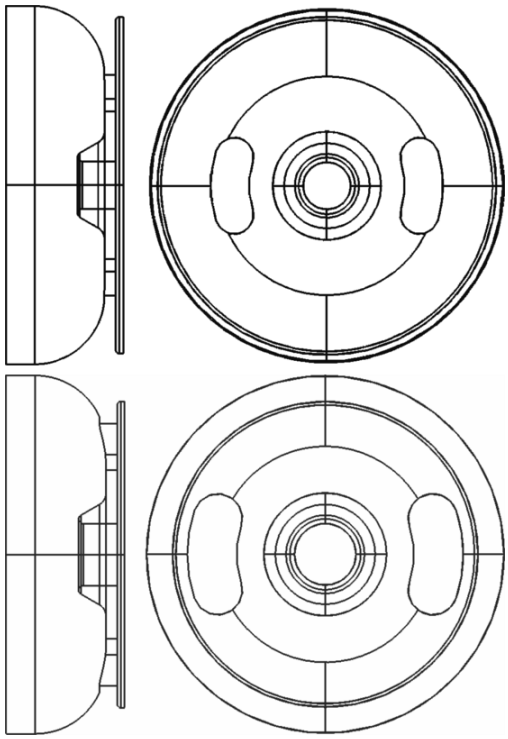

Figure 1: Profile of the MAMI Ilac (top) and of the MAMBO (bottom).

The numbers of cell coupling k, k_1 and k_2 and passband gap δ have been obtained from five parameter DISP-fits [5]. The frequencies to be fitted to the dispersion function have been taken from CST microwave studio (MWS) simulations. The parameters are $k = 8\,\%$, $k_1 = k_2 = 0.9\,\%$ and $\delta = 1.9\,\mathrm{MHz}$. A three parameter DISP-fit leads to $\delta = 0.7\,\mathrm{MHz}$ and $k = 8\%$.

In course of the design process the complete RF-sections have been modelled within CST Studio Suite. Also special cells for RF-input, tuner and the end groups were considered. To tune those cells to the correct frequency, the cell radii had to be adjusted. The input and tuner cells have a slightly smaller radius than the standard cell, the end group has a larger radius. For the graded-β section of course each cell had to be tuned. Tuning of frequency can be achieved by either changing the radius of the cell or by cutting off the tips of the nose cones.

The field pattern of the $\beta = 1$ structure including all special cells is plotted in Fig. 2. As one can see the field is adequately flat. The absence of field inside the short coupling cells hints to a sufficiently closed passband gap.

The results of the MWS simulations of all RF-sections of MAMBO are listed in Table 2. Since the RF-input coupling is realised by slots the coupling strength κ is fixed, thus it is optimised for a maximum beam loading of 10 mA. The RF forward power needed to support a field gradient of 1 MV/m at zero current is with this coupling at least 40 kW. The shunt impedance of a low beta structure is considerably lower, so more than 62 kW will be necessary to maintain 1 MV/m in the graded-β.

Table 2: Data of the MAMBO RF-sections

		S1	S2	S3&4
β		0.548 - 0.957	0.977	1
L	[mm]	1658	1689.5	1729.5
R/Q	[Ω]	2309	3810	3886
Q_0		21500	23600	24000
R_s	[MΩ]	49.7	90.2	93.3
κ		1.27	1.46	1.45
E_0	[MV/m]	1.0	1.0	1.0
P_c	[kW]	50.6	31.6	32.1
$P_{g,0\,\mathrm{mA}}$	[kW]	62	39.3	39.5
$P_{g,10\,\mathrm{mA}}$	[kW]	75	53.1	53.3

THERMAL DESIGN

With thermal losses of the order of 20-30 kW/m inside the copper of the RF-structures sufficient cooling of the linac sections is needed. Heating of the nose cones is crucial since it can lead to a permanent detuning of the structure eventually causing damage beyond repair. While water cooling of the cavity shell is easy to calculate, for cooling of the nose cones by thermal conduction through the web numerical calculation is useful. The design goal is to have the temperature of the nose cones well below 70°C.

The thermal simulations were performed with the multi-physics solver (MPS) of CST Studio Suite using the field data of MWS as input. Further it is necessary to define emissivity and heat transfer coefficient α of the thermal surface, i.e. the cooling channels. The emissivity of a copper surface is approx. 1%, α depends on the geometry of the surface.

$$\alpha = \frac{N_{\mathrm{Nu}}\lambda}{d_{\mathrm{chan}}} \tag{1}$$

With N_{Nu} being the Nusselt number, λ the thermal conductivity of the coolant and d_{chan} the diameter of the cooling channel. The Nusselt number is a function of the Prandtl number N_{Pr} and the Reynolds number N_{Rey}:

$$N_{\mathrm{Nu}} = C \cdot N_{\mathrm{Pr}}^{n} \cdot N_{\mathrm{Rey}}^{m} \tag{2}$$

For a coolant flowing through pipes the parameters are: $C = 0.023$, $n = 0.4$ and $m = 0.8$ [6].

$$N_{\mathrm{Pr}} = \frac{\nu c_p \rho}{\lambda} \tag{3}$$

The quantities in N_{Pr} are: ν the viscosity, c_p the heat capacity and ρ the density of the coolant. The Reynolds number is given as:

$$N_{\mathrm{Rey}} = \frac{v \cdot d_{\mathrm{chan}}}{\nu}, \tag{4}$$

v is the velocity of the coolant. The flow of the coolant can be determined by:

$$\dot{m} = \frac{P_c}{c_p \Delta\theta}, \tag{5}$$

P_c is the power lost in the cavity walls (see Table 2) and $\Delta\theta$ the temperature change of the coolant.

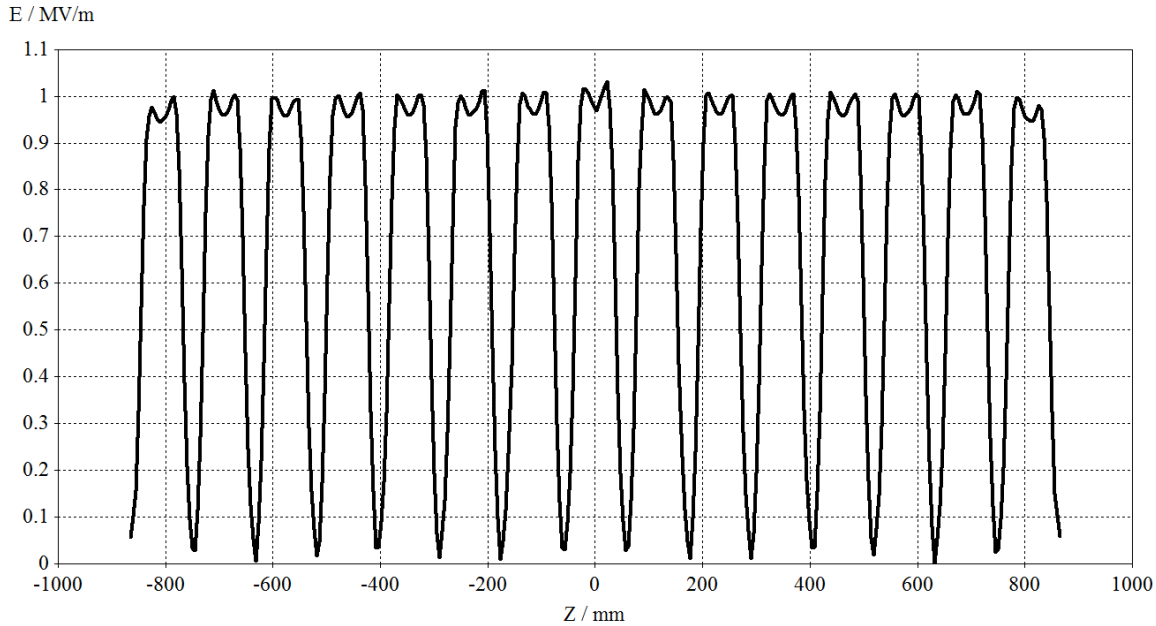

Figure 2: The field pattern of the $\beta = 1$ RF-section. The strong cell coupling produces a very even field distribution that only drops a little in the end cells. The field peak in the centre is due to the input coupling there.

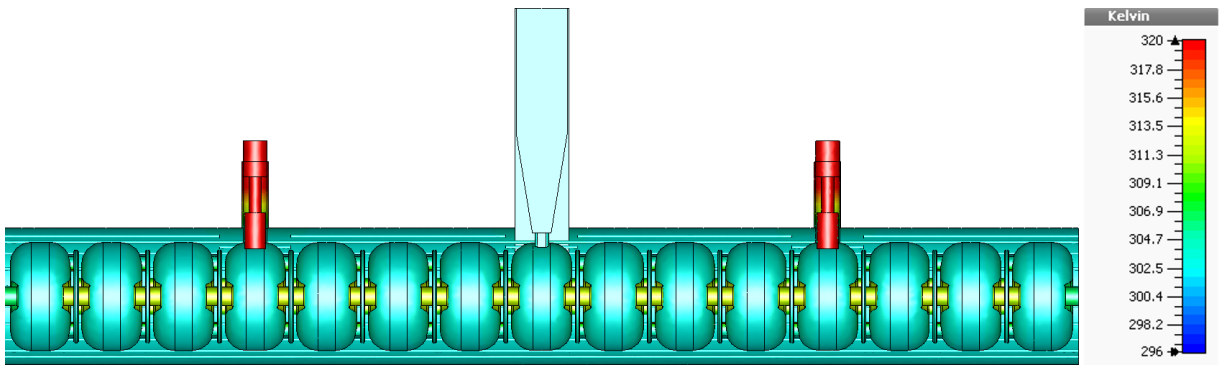

Figure 3: The thermal simulation of the $\beta = 1$ structure as example. With the given design the iris temperature is $\theta \approx 40°C$. The plungers can have a temperature of up to 80°C if they are fully moved inside the cavity without cooling. The temperature scale is cropped at 320 K to provide a better resolution of low temperatures.

Assuming a temperature change of ca. 10°C and water as coolant ($N_{Pr} \approx 6.7$), the flow of coolant must be $\dot{m}_{H_2O} \approx 55\,L/min$ to match the thermal load of the cavity. A variation of number and diameter of cooling channels gave optimum α at 20 cooling channels having a diameter of $d_{chan} = 5\,mm$, then $\alpha \approx 1\,W/(K \cdot cm^2)$ for a wide range of thermal loss.

The heat distribution of the MPS simulation for $\theta_{room} = 23°C$ and $\theta_{H_2O} = 28°C$ of the above configuration can be seen in Fig. 3. The temperature of the nose cones is approx. 40°C, which is well below damage level.

SUMMARY

The design of MAMBO has improved. Beam dynamics simulations have become more realistic due to an improved number of levels of the research. The RF-design of the accelerating structures is nearly finished, as well as thermal design. The process of mechanical design has been started.

REFERENCES

[1] R. Heine and K. Aulenbacher, "Injector for the MESA Facility", in *Proc. IPAC'13*, Shanghai, China, May 2013, p. 2150.

[2] H. Euteneuer *et al.*, "The Injector Linac for the Mainz Microtron", in *Proc. EPAC'88*, Rome, Italy, Jun. 1988, p. 550.

[3] L.M. Young, "PARMELA", Los Alamos, USA, LA-UR-96-1835, (2005).

[4] CST - Computer Simulation Technology, Darmstadt, Germany.

[5] S.O. Schriber, priv. communication, (2002).

[6] W. Beitz, K.H. Grote (ed.), "Dubbel - Taschenbuch für den Maschinenbau", 20th ed., Springer (2001)

ISBN 978-3-95450-168-7